Limnol. Oceanogr., 43(5), 1998, 946–954

Stability and meromixis in a water-filled mine pit

C. L. Stevens[1] *and G. A. Lawrence*
Environmental Fluid Mechanics Group, Department of Civil Engineering, University of British Columbia, V6T 1Z4 British Columbia

Abstract

A field experiment examined stability and stratification in a disused mine pit filled with 1.75×10^7 m^3 of water. Vertical profiles of conductivity and temperature indicated that, due to substantial chemical stratification, spring and autumn overturn did not penetrate to the base of the pit. Although parameterization indicated that double diffusion should be expected, we found only circumstantial evidence of associated step structure. The available data suggest that groundwater inflow created a warm salty pool of water at the base of the water column, giving the appearance of a meromictic structure with a monimolimnion. However, this pool was not a consistent feature, suggesting both a variable inflow and significant diffusion rates. From the temperature data, estimates indicated that hypolimnetic vertical eddy diffusivity varied between 1×10^{-7} and 5×10^{-5} m^2 s^{-1}. The observations identify short-term relatively energetic internal wave events that may have a significant impact on this value. The present study is useful in two ways: first, it shows how pit-lakes form a natural laboratory for a range of processes, and second, it illustrates how these processes relate to diffusion parameterization. It is clear that reliable parameterization is vital for long-term modeling required for prediction of water quality over decadal timescales.

With the closure of an open-cut mining operation come the dual problems of rehabilitation of the mine pit and containment of deleterious material generated by the mine during its life. In many cases the pit fills with water, either naturally or through mine activities. Thus, an artificial lake of moderate volume is created (Davis and Ashenberg 1989). Characterization of the transport processes within the water column is important for two reasons. First, the pit is likely to contain hazardous levels of dissolved metals, and second, if vertical transport rates are low then the pit may prove suitable as a storage location for hazardous material.

Water-filled mine pit lakes ("pit-lakes") have received consideration in the literature but with a biological or geochemical emphasis (e.g. Klapper and Schultz 1995). Crater lakes are the natural system most similar to these artificial water bodies (Martin 1985; MacIntyre and Melack 1985). Pit-lakes are unique for several reasons: they are often deep relative to natural lakes of similar surface area; they have high surrounding walls that often generate a microclimate different to that outside the pit; they typically have very thin sediment layers; they may undergo substantial and rapid changes in water level; and they are likely to contain significant concentrations of dissolved material. The final point is important if the dissolved material is environmentally harmful or if it leads to meromixis. With these departures from what might be associated with typical natural lakes, field observations are required to examine the basic hydrodynamics of pit-lakes.

The present paper describes certain factors affecting vertical transport in mid-latitude pit-lakes. Emphasis is placed on effects, such as under-ice double-diffusion, that are less frequently observed and described in limnological literature. This serves a dual purpose. First, the mechanistic prediction of vertical transport rates in pit-lakes is fundamental to reliable long-term modeling of water quality (e.g. Stevens and Lawrence 1997*a*; Hamblin et al. 1997). Second, pit-lakes can provide a relatively ideal natural laboratory to examine particular processes.

Site description and equipment

The field observations were recorded in the Brenda Mines pit-lake 40 km west of Kelowna, British Columbia (49°53′N, 120°00′E) at an elevation of 1,450 m. The pit, originally mined for molybdenum, was closed in 1990. Cessation of dewatering at that time resulted in a steady filling of the pit, so that by mid-1995 the water in the pit was >140 m deep and ~700 m in diameter at the surface (Fig. 1). Most of the inflow was pumped from a nearby shallow tailings pond, with additional water sources including two small streams, direct precipitation, site runoff, and groundwater. The bathymetry and topography was more complex than the 25-m isopleths in Fig. 1 suggest, as the walls, both above and below the water surface, were formed by ~10-m-high mine benches. This resulted in a stepped bathymetry. Typically, the pit-lake is ice-covered for 6 months of the year (e.g. 25 November 1994–7 May 1995), with maximum ice thicknesses >1 m and snow depths of 0.5 m.

Routine water quality data, including chemical composition and coarse (10-m vertical interval) thermal and dissolved oxygen data, have been collected since the commencement of filling. As part of the intensive sampling in the present study, CTD profiles were recorded with an Ocean Sensors 200 CTD (temperature and salinity resolution of

[1]Present address: National Institute of Water and Atmospheric Research, P.O. Box 14 901 Kilbirnie, WGTN New Zealand.

Acknowledgments

We thank Tom Murphy (Canadian National Water Research Institute) for the loan of equipment and Heather Larratt and Derek Perkins for water chemistry and bathymetry data. The work was funded by Environment Canada, CANMET, and Brenda Process Technologies. The UBC Environmental Fluid Mechanics Group graduate students provided field support. We also thank Paul Hamblin, Rob McCandless, Bill Price, Bonnie Marks, Sally MacIntyre, Carolyn Oldham, three anonymous reviewers, and the editor for contributions to this paper.

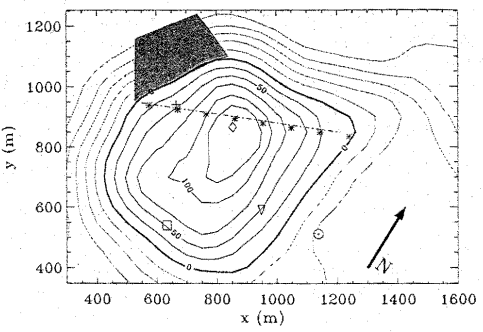

Fig. 1. Contours of the topography above and below the water surface at 25-m intervals—surface station (◇), observation station (⊙), profile locations C1 (+) and C2 (□), side thermistor chain location (▽), and the dashed line marks a CTD transect line of profiles at 100-m intervals (*). The shaded area is a region of wall collapse.

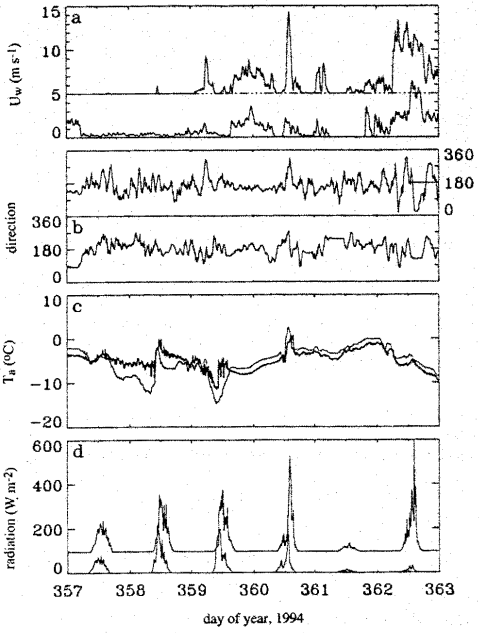

Fig. 2. Comparison of meteorology data from two stations, including (a) wind speed at surface station and observation sites, with the latter offset by 5 units, and both records averaged over 10-min intervals; (b) wind direction with hour-long averages, with the observation station in the upper panel; (c) air temperature with the observation station denoted by the thicker line; and (d) incoming solar radiation, with the observation station offset by +100 W m^{-2}.

0.01°C and 0.01 PSU, respectively) approximately monthly from March 1994 through September 1995. The recording of most profiles took place at the point over the deepest region of the pit-lake (surface station, *see* Fig. 1). Meteorological data (Young anemometers, Rimco pyranometers, Väisälä Relative humidity/air temperature sensors) were recorded at the observation station on the edge of the pit wall, 50 m above the water surface (*see* Fig. 1), for the period from 21 October 1994 until the end of May 1995. Similar data were collected for a total of 23 d (20–25 December 1994 and 21 January–6 February 1995) by a meteorological station on the ice surface at the same location as the CTD profiles. The two stations were 500 m apart horizontally. Thermistor loggers (TSKA WaDaRs and Brancker TR1000s, resolution of ~0.005°C) were deployed in various configurations to capture high-frequency thermal variations from September 1994 until July 1995.

Results

Meteorology—The air temperature at the site varied from the mid-20s°C during summer to less than −20°C in winter. The area was subject to periods of heavy fog, resulting in minimal incoming radiation for extended periods. Wind events in the region were most energetic during autumn storms. The maximum 15-min average wind speed recorded was 12 m s^{-1} observed at the observation site. The wind speed at the pit-lake surface was ~70% of that at the observation point.

Because of the topography, care needs to be taken when applying meteorological data recorded outside the pit to those acting at the pit-lake surface. Based on a 6-d section of data (Fig. 2a–d), recorded simultaneously during winter at the surface and observation stations, it appears that the micro-meteorology within the pit walls was markedly different from that only a short distance away outside the pit (Fig. 1). Modeling based on data from even close by the pit-lake, while easier to obtain, would lead to significant errors in estimates of heat fluxes and stress transfer.

Water balance—Compiling a mass balance for the pit-lake, despite it having no known outflow, was not trivial. The budget consists of precipitation, runoff, stream inflow, groundwater inflow, and mine pumping rates, all derived from mine reports (Brenda Mines pers. comm.). Figure 3 shows the volume–height curve interpolated from topographical data (▽). Estimates of the water collected are included as an end-of-year elevation. By the end of 1995 the water balance level was 5 m lower than the observed level. Although this is only a 3% error in elevation, it represents almost a 10% error in volume. It is possible that a significant portion of the observed and estimated volume difference is due to uncertainty in the bathymetric data.

Precipitation (including evaporation) and surface runoff can all be estimated from observations (e.g. totals for 1994 were 123 × 10^3 and 204 × 10^3 m^3, respectively). Mine pumping is by far the largest component of this balance,

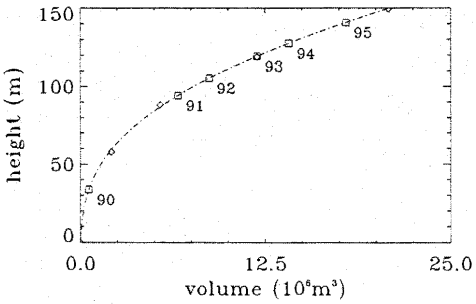

Fig. 3. The water mass balance. □, Indicates the calculated volume at the end of each year; ◇, observations at various times; -·-·-, curve fitted to the calculated volume data.

accounting for ~80% of observed inflow (e.g. the total for 1994 was 1.57×10^6 m³). The bulk of the pumping occurred just after ice-off, where water was pumped from a nearby but relatively warm shallow tailings pond (average depth of ~3 m). Water entered the epilimnion, reducing the overall clarity significantly due to its turbidity (Secchi depth decreasing from >12 m prior to pumping to ~3 m).

The information known about the groundwater inflow was largely derived from a consultants report (Klohn Leonoff 1986) written prior to the mine closure. The estimation of groundwater inflow into the pit prior to filling suggested an average rate of 8 liters s^{-1} (i.e. 252×10^3 m³ annually). This water had no single source but rather came from fissures of various sizes and at various heights in the pit walls. The flow rate was likely affected by the filling of the pit, but as the present water level is still >100 m below the original water table, this prefilling flow rate represents a useful post-filling estimate. A consequence of the stratification is that, while the groundwater forms a secondary part of the mass balance (10%), it may generate significant effects at depth as it enters the water column and moves to its level of buoyancy equilibrium.

Profile data—Variations in the temperature and salinity structure are illustrated in the compilation of profiles shown in Fig. 4. These profiles, spanning 18 months, clearly show the initial under-ice surface layer that warmed, forming a wind-mixed epilimnion with temperatures >12°C. The temperature structure reveals two regions where the water column was unstable with respect to the temperature component of the equation of state. These regions were just beneath the epilimnion and at the very base of the water column. As the pit-lake retained consistent thermal and conductivity structure from month to month, it was assumed that the pit was not continually unstable and that chemical stratification maintained overall stability. Typical concentrations of major ions (150 mg liter^{-1} of Na^+, 150 mg liter^{-1} of Ca^{2+}, 201 mg liter^{-1} of Cl^-, and 436 mg liter^{-1} of SO_4^{2-}) were such that temperature compensation of the conductivity reading, in conjunction with the assumption that salinity is proportional to temperature-corrected conductivity (Wüest et al. 1992), enabled density to be inferred from in situ conductivity measurements (Chen and Millero 1977). This process can be considered in detail by examining the CTD data recorded on 20 October 1994 and shown in Fig. 5. The temperature (Fig. 5a) was everywhere greater than the temperature of maximum density (~4°C at the surface, decreasing to ~3.7°C at the pit-lake base), with a marked increase in the vertical temperature gradient in the deepest 10 m of the profile. The temperature near the pit-lake bottom was 1°C greater than the temperature of the water 30 m above the bottom. The in

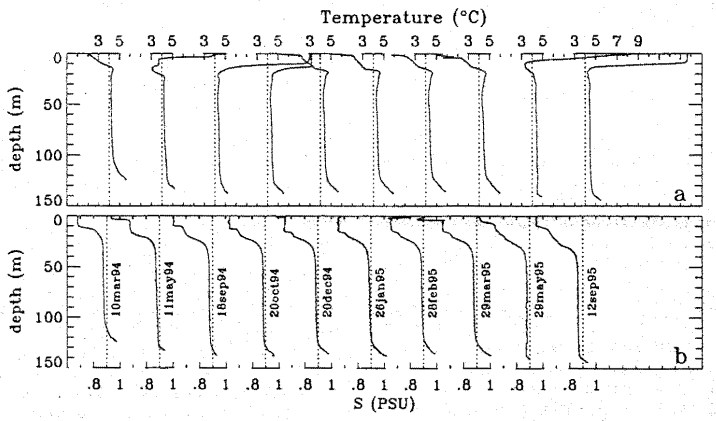

Fig. 4. (a) A sequence of temperature profiles, where the vertical dotted line indicates 4°C for each profile. (b) A sequence for salinity, where the vertical dotted line indicates the 0.9 PSU level. The profile dates are as indicated in panel b.

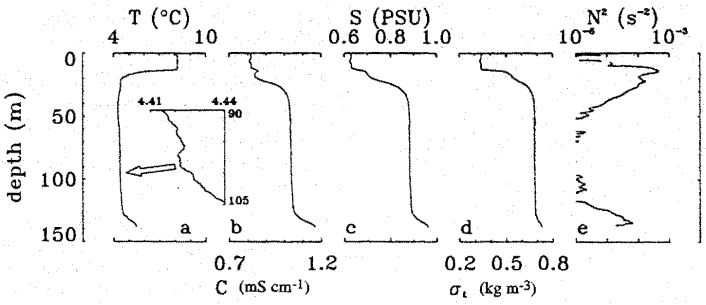

Fig. 5. CTD profile recorded 20 October 1994 showing (a) temperature (and an inset of an expanded segment), (b) in situ conductivity, (c) salinity, (d) density, and (e) buoyancy frequency squared.

situ conductivity profile (Fig. 5b) clearly illustrates the sensitivity of conductivity to temperature; the spike at 13-m depth was not a sensor mismatch, but evidence of the rapidly changing temperature. The method for salinity determination described above was applied so that the spike was compensated for (Fig. 5c) and the resultant potential σ_t profile (density $-1{,}000$ kg m^{-3} relative to 0 m, Fig. 5d) is stable, apart from some patches in the very surface layer and some very low amplitude noise. The buoyancy frequency, a measure of stability, is given by

$$N^2 = -\frac{g}{\rho_0}\frac{\partial \rho}{\partial z}, \tag{1}$$

where g is gravitational acceleration, ρ_0 is a reference density of the water, and $\partial\rho/\partial z$ is the vertical gradient of density relative to pressure at 0 m. N reached values $>5 \times 10^{-2}$ s^{-1} (Fig. 5e), although a combined calibration error of about $\pm 10\%$ must be expected. This value for N provided a basis for selection of thermistor chain sample frequencies.

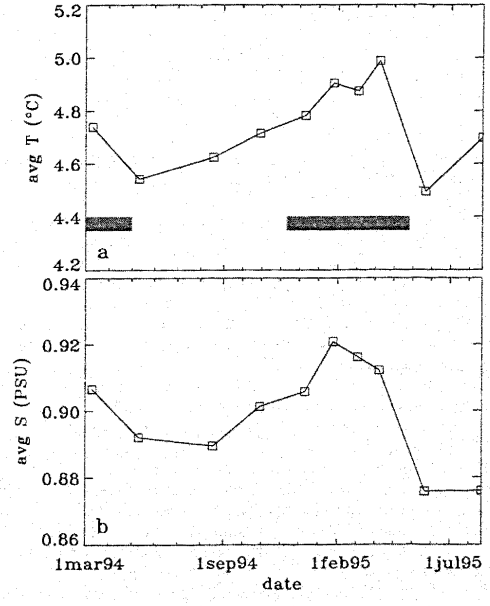

Fig. 6. Area-weighted, vertically averaged (a) temperature and (b) salinity in the deepest part of the water column. The horizontal bars in panel a represent periods of ice cover.

The temperature and salinity profiles show the warm salty layer at the bottom of the pit-lake (Fig. 4). This normally would be a clear indicator of meromixis; however, there seems to be a seasonal cycle where the overall excess heat and salt decreases rapidly around March in both 1994 and 1995. Figure 6a and b show the areally weighted heat and salt budgets for the bottom 20 m of the water column, including the two March decreases in heat and salt. The average temperature rose from 4.45°C to almost 5.0°C while the average salinity rose from 0.89 PSU to a peak of 0.92 PSU in the period September 1994 through March 1995. Temperature increased monotonically through this time, but salinity peaked in January and then decreased slightly. Because this signal cannot be generated by geothermal heating owing to changes in salinity, we assume that it is generated by the groundwater inflow observed before filling of the pit.

Temperature time-series in the absence of ice cover—Temperature time-series provided high temporal resolution information that were aliased in monthly profiles. The general observation for the ice-free months was that, even though the wind field acting at the water surface was attenuated by the pit walls and was more variable than that experienced outside the pit, there was still sufficient energy to drive internal waves. Figure 7a shows deflections inferred from a section of the 10-m thermistor data using a nearby temperature profile. The time-series was recorded at the "side-station" (*see Fig. 1*) just prior to when the surface

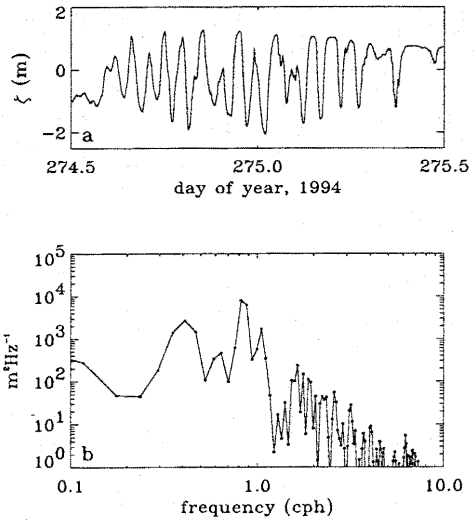

Fig. 7. (a) Vertical displacement inferred from a section of the 10-m-deep thermistor time-series at the side station (∇ in Fig. 1), recorded on the 1 and 2 October 1994, and (b) the power spectral density of this record.

layer deepened to 10 m. These waves produce peak-to-peak excursions >3 m. The power spectral density of this record (Fig. 7b) indicated two strong peaks, suggesting that the first mode baroclinic period was 1.25 h and the second mode was 2.5 h. A two-layer, two-dimensional estimate of the first mode period is given by

$$\frac{2L}{\sqrt{g' h_1 h_2/(h_1 + h_2)}}, \tag{2}$$

where L is the average width of the basin at the depth of the thermocline h_1 overlying a layer of average depth h_2. The reduced gravity ($g' = \Delta\rho g/\rho_0$) incorporates the density step at the thermocline $\Delta\rho$. In the present system, estimates of the variables (L of 600 m, $\Delta\rho$ of 0.62 kg m^{-3}, h_1 of 15 m, and h_2 of 75 m) results in a period estimate of 1.2 h. Estimations of these oscillations are important for boundary-mixing predictions (Hamblin et al. 1997).

Temperature time-series in the presence of ice cover—Ellis et al. (1991) suggested that, after the onset of ice cover and when air temperatures are <0°C, under-ice-water temperature fluctuations should be minimal and involve slow diffusive changes in temperature almost at molecular rates. The temperature observations recorded in February, when air temperatures were well below 0°C, show a different picture. Figure 8 shows air temperature and eight temperature time-series spanning the period between profiles 6 and 7 (26 January–28 February 1995) of Fig. 4. All temperature records differed—the 10-m thermistor exhibited a high frequency oscillation that was much more rapid than the daily heating cycle, whereas the 15-m sensor, which lay at the point of maximum stability, recorded two pulse-like temperature changes of ~0.06°C. Note the disturbance that occurred late in the record around day 56.5. Close examination of the air-temperature data (Fig. 8a) revealed that this burst occurred just after the air temperature dropped below 0°C, suggesting that the thaw–freeze processes may have loosened an unstable part of the mine-pit wall, which slid into the pit.

The general displacement amplitudes of the fluctuations decreased with depth except at 130 m. Water at this depth warmed markedly over the month and was subject to several events (not seen elsewhere) that were shocklike in structure; that is, they had a very sharp front and a decaying oscillatory tail as illustrated in the expanded inset of (Fig. 8i). The times of the events in the 130 m record are shown as vertical dashed lines in the other time-series. These events did not manifest themselves at any other location in the water column. Two potential explanations are either that the events were generated by wall slippage that occurred beneath the 80-m sensor or that the very low temperature gradient at 80 m (~0.001°C m^{-1}) was insufficient to generate measurable temperature changes. If the event had caused perturbations at the higher locations (60 and 40 m), the elevated temperature gradients (which were 3.7 and 2.8 times greater than at the 80-m position) would have resulted in measurable temperature changes. In addition, the bathymetry must serve to concentrate any downward-moving event as the pit radius is roughly 50 m at the bottom, compared to the surface radius of 350 m. The temperature increase in Fig. 8i does not agree with the temperature budget of Fig. 6a, and it is assumed that this is due to aliasing of the temperature structure with monthly profiles. Variation in the temperature (and salinity) structure at the time of the February profile may have been associated with the moderate level of activity observed in the 130-m sensor after day 56.5—fluctuations caused by the event discussed above.

The high-frequency temperature fluctuations in the upper water column with ice-cover (Fig. 8b–e) were unrelated to air temperature, leading to the hypothesis that they were due to groundwater and(or) surface-water fluxes. These temperature fluctuations are elucidated by a horizontal transect of CTD profiles recorded at 100-m intervals early in March 1995 (Fig. 1). The transect revealed patches of water at the edges of the pit in the surface layer that were fresher and colder than at the center of the pit. Figure 9a shows the difference between the local temperature profiles recorded on the transect compared to the central profile, with each profile being offset, and Fig. 9b shows similar data for the salinity. Colder, fresher water is indicative of surface runoff during winter. The low correlation between the air temperature and the upper water-column temperature fluctuations that have periods of around a week (Fig. 8c) must therefore be related to the hydrological processes releasing the inflow in the first place.

The buoyancy differences associated with the inflow generates inward-flowing intrusions because of the quite substantial horizontal density gradients. The upper 5–10 m of the water column were ~0.15 kg m^{-3} lighter away from the

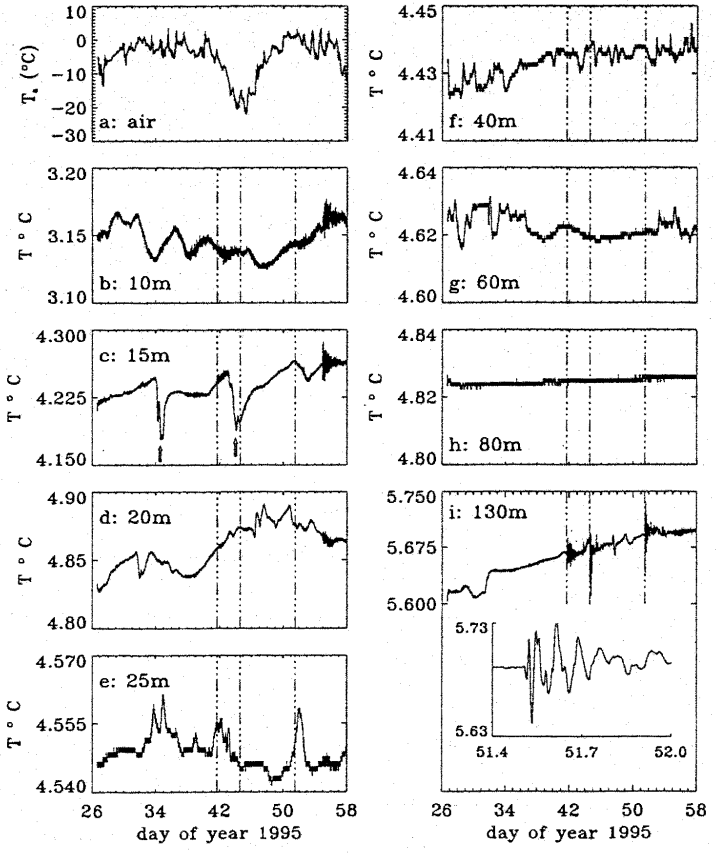

Fig. 8. Under-ice temperature showing (a) air temperature and (b–i) temperature records from depths of 10, 15, 20, 25, 40, 60, 80 and 130 m—note the different temperature scales and the resolution limit in panels e–h. The arrows in panel c indicate two cold pulses while the dashed lines are for time registration of the events in panel i. An expanded inset of one of the sudden events is also included in panel i.

lake center, and the intrusion at a depth of ~20 m was ~0.01 kg m^{-3} lighter. Intrusion velocities are described by

$$u_i = (2g'\delta)^{1/2} \quad (3)$$

(Turner 1973), where g' is the modified gravitational acceleration associated with the density difference, and δ is the intrusion thickness. For the two levels of inflow captured in Fig. 9 we selected δ of 4 and 3 m, respectively, and the density differences imply g' of 15×10^{-3} and 1×10^{-4} m s^{-2}. The calculated velocities are then 0.11 and 0.02 m s^{-1}. These estimates suggest that transport from the edge to the center of the lake at the surface can occur in as little as an hour.

Discussion

Turnover and meromixis—Fundamental questions when considering long-term vertical mixing in temperate lakes are does turnover occur, and if so, how far does it penetrate? The Brenda pit-lake differs from most natural lakes owing to its significant salinity stratification. Turnover does not occur in this system because the salinity stratification at the

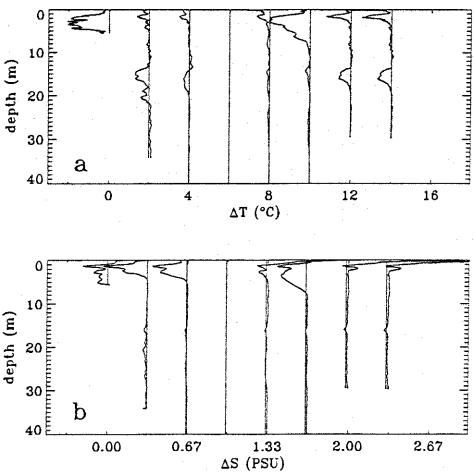

Fig. 9. Data from a transect of under-ice CTD profiles recorded on 1 March 1995 over a period of 2 h showing (a) the temperature profile minus the central temperature profile, so that a negative temperature difference means that the side water is colder (each profile is offset by 2°C), and (b) similar salinity data with each profile offset by 0.33 PSU.

base of the epilimnion is too strong. Evidence of this is found in the salinity and temperature profiles, which remain largely unchanged just beneath the epilimnion at the expected time of turnover despite having substantial structure. Stevens and Lawrence (1997*a*) illustrated the difference between the present system and turnover in a natural lake. Additionally, the temperature profile in the hypolimnion does not decrease to the temperature of maximum density, and regular dissolved oxygen profiling by the mine operators (H. Larratt pers. comm.) did not find substantial changes in dissolved oxygen beneath the epilimnion. Also, Hamblin et al.'s (1997) modeling of this dataset found that there was insufficient energy to mix the epilimnion beneath 19 m. This lack of turnover has far-reaching consequences for the transport in the pit lake. Because the pit-lake is not dimictic, it is potentially meromictic. The temperature and salinity profiles result in an instantaneously stable density profile (e.g. Fig. 5d) that gives the appearance of a meromictic lake. However, the opposing salt and heat gradients provide suitable conditions for double diffusion.

Double diffusion—Heat diffuses ~100 times more rapidly than does salt, so that the warm, salty, stable layer loses heat more rapidly than does salt. This results in the hypolimnetic fluid adjacent to the warm salty layer becoming lighter. The density structure is such that the new level of neutral buoyancy for this fluid is at the base of the surface layer, 100 m higher in the water column. The mixing that ensues as the fluid tries to move to this new level of neutral buoyancy raises the apparent K_z. Geothermal heating has a somewhat similar effect (Newman 1976; Wüest et al. 1992), but without the salt flux. Wüest et al. (1992) explored the stability of the double-diffusion region by examining the relative positive and negative contributions to stability, N^2, by heat and salt. The relative effects are quantified with the ratio

$$R_\rho = \frac{\partial \rho_S}{\partial z} \Big/ \frac{\partial \rho_T}{\partial z}, \tag{4}$$

where ρ_S and ρ_T are the relative contributions to density through salinity and temperature (with an overall expected error of ±5%). Figure 10 shows scatterplots of the resulting R_ρ for the profiles of Fig. 4. The first profile was recorded at half the sampling frequency of subsequent profiles, resulting in poorer spatial resolution (the gradient operation amplifies the noise in all panels). However, the general

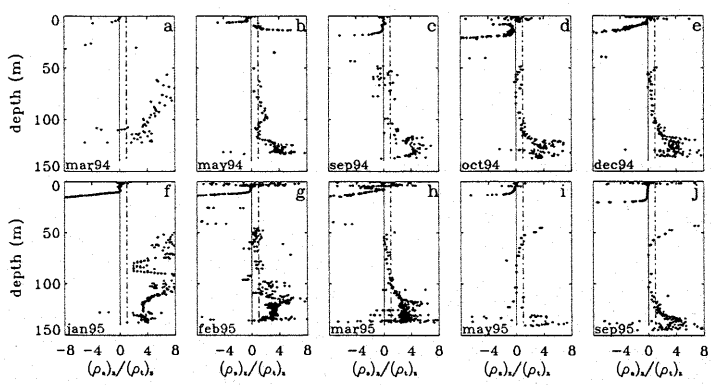

Fig. 10. Profiles of the stability comparator, R_ρ, where each profile is in the same sequence as that presented in Fig. 4a and b as indicated by the month and year.

trends are clear. The epilimnion generally sits around R_ρ of 0, and underneath R_ρ drops to negative values, well offscale, indicating strong stratification in both T and S. By ~45–55 m, R_ρ returns to near-zero values, indicating that from ~50 to 110 m we should expect an essentially unstratified environment. Beneath this, conditions appear acceptable for double diffusion. Similar to McManus et al. (1992), we found no clear evidence of the telltale step structure (Newman 1976); however, we did find possible remnants of such events. The inset in Fig. 5a shows a section of the temperature profile indicating pulses of water with anomalous temperatures. The temporal variability in the R_ρ profiles is consistent with the idea of sporadic double diffusion. None of these observations are consistent with slow molecular diffusion.

The variability is amply illustrated by the apparent seasonality of the deep inflow. The CTD profile of late May 1995 (second to last profile of Fig. 4) indicated that the deep salty pool no longer existed. Numerical solutions to the equation

$$\frac{\partial S}{\partial t} = \frac{1}{A}\frac{\partial}{\partial z}\left(K_z A \frac{\partial S}{\partial z}\right), \tag{5}$$

where S is the salinity of material being considered and A is the cross-sectional area as a function of depth z, found that $K_z \approx 5 \times 10^{-5}$ m^2 s^{-1} best matched the observations. This is greater than empirical estimates based on Heinz et al. (1990) and Hondzo and Stefan (1993), which are more likely around 1×10^{-6} m^2 s^{-1}. The vertical lengthscale based on the eddy diffusion suggests that in a time t the groundwater will spread over the deepest $(K_z t)^{1/2}$ m, so that in 6 months the groundwater layer grows to a thickness of ~30 m, which is comparable with the observations. Furthermore, averaging over this vertical scale, and if we assume that the inflow is a constant 8×10^{-3} m^3 s^{-1}, then we can estimate the inflowing temperature and salinity to be 5.7°C and 0.95 PSU.

An additional estimate of vertical eddy diffusivity may be garnered by the gradient flux method whereby Fick's law of diffusion is used to find the required eddy diffusivity to generate the observations (*see* e.g. Jassby and Powell 1975; Heinz et al. 1990). Substantial time-averaging of the raw data was required to determine consistent eddy diffusivities; a month-long average indicates that the eddy diffusivity at 80 m was $\sim 2 \times 10^{-5}$ m^2 s^{-1}. Note that this diffusion results in a warming due to the inflow at the pit-lake base as opposed to a cooling that might normally be expected with wintertime top-down processes. This is somewhat less than eddy diffusivity estimates in the fluid directly above the warm salty layer, but is still an order of magnitude greater than the empirical estimates mentioned above. Additionally, in this study the gradient flux technique was only applicable at this depth (80 m), as applying the approach at other locations in the water column resulted in negative calculated values for eddy diffusivity. In other words, the scale at which transport occurred was comparable to or greater than that over which Eq. 5 (but replacing S with temperature) was considered. External events may have transported heat to a depth of 80 m, so that the fluid there increased in heat content regardless of adjacent thermal gradients. This up-gradient transport represents an inappropriate use of the eddy diffusion model since the scale of the mixing is greater than the discretization used. Groundwater fluxes, turbidity currents due to wall subsidence, and turnover are possible external effects that can lead to such large-scale motion.

Internal waves—The short surface and internal seiche timescales (O [1 min], O [1 h], respectively) imply that even variable winds can generate pressure gradients to drive internal waves. A broad spectrum of internal waves is a ubiquitous feature in stratified basins. Typically, the basin-scale components of this spectrum are of greatest importance. Basin-scale internal waves of even moderate amplitude may cause boundary mixing (Wüest et al. 1996). Furthermore, if the waves are of sufficient amplitude to bring the base of the epilimnion to the surface, then upwelling and enhanced entrainment occur (Monismith 1986). Estimates of basin-scale internal wave amplitudes in the Brenda pit-lake using the Wedderburn number (Stevens and Lawrence 1997*b*) indicate that, even at the time of weakest stratification, the wind causes vertical excursions of the interface of only a few meters (e.g. Fig. 7a). Although upwelling of the interface to the surface is thus unlikely, this does not mitigate the effects of the internal seiche-driven benthic boundary layer. Because the tilt implied by the Wedderburn number should occur in one-quarter of the first-mode internal seiche period, the resulting horizontal velocity in the hypolimnion can be estimated. Some of the stronger wind events recorded in this study should have generated velocities of 0.015 m s^{-1} at the bottom of the water column. This has the potential to generate enhanced mixing (Hamblin et al. 1997).

The mixing effects of the under-ice internal waves are more difficult to quantify since their spatial scale is not resolved in the observations. It is apparent that they must lead to continual motion high in the water column but are confined to irregular but substantial events at the base of the pit-lake. Any motion at these depths with weak stability will enhance vertical diffusion by sharpening gradients. The inset in Fig. 8i shows an expanded section of the 130-m thermistor record, which represents ~0.5-m vertical excursions over ~30 min. Although recorded in the pit-lake center, if the magnitude is taken to represent the sidewall deflection, and the monimolimnion is taken as 5 times wider than the depth, then the shear at the monimolimnion–hypolimnion interface can be estimated. This suggests an approximate gradient Richardson number ($\mathrm{Ri}_g = N^2/(\partial u/\partial z)^2$) of 20. Münnich et al. (1992) related eddy diffusion to Ri_g, suggesting that K_z equals 1×10^{-7} m^2 s^{-1} for the present estimation of Ri_g. This diffusion coefficient is two orders of magnitude greater than molecular diffusion of salt. Three such internal-wave events were identified in the month-long data record of Fig. 8, indicating that they are not anomalous.

A concluding seasonal picture

In summer, warm air temperatures in the British Columbia interior and the sheltered micro-meteorology result in an strongly stratified epilimnion owing to temperature and to the perennial salinity-related stratification. Despite shelter-

ing, wind action at the water surface is still substantial enough to generate internal waves of several meters amplitude at the thermocline. Although this is insufficient to upwell the hypolimnion, it must drive benthic motion, presumably leading to enhanced vertical diffusion. With the approach of autumn, the loss of thermal buoyancy is insufficient to overcome the salinity stratification, and turnover does not occur. At this time the Brenda pit-lake differs from most lakes at similar latitudes, as the top-driven penetrative convection is confined to only a portion of the water column. However, the salinity stratification can lead to double-diffusion effects. Conditions were found to be suitable for double diffusion, but only weak evidence of its effect was found.

Whereas the onset of ice cover does stop wind-driven internal waves there are other driving mechanisms that become more apparent, including groundwater and surface runoff. In addition, sporadic shocklike events, which we speculate are wall-subsidence related, generate substantial motion deep in the hypolimnion. All these processes must lead to eddy diffusivities well in excess of molecular diffusion rates. The winter processes observed here were much more complex than expected and suggest that more effort should be placed on observations during this time.

As with autumn, the buoyancy effects due to the warming surface waters during spring were insufficient to overcome the salinity stratification at the base of the epilimnion, and so the pit-lake does not go though spring turnover. This normally would mean that the pit-lake is meromictic by definition. The deep, warm, salty pool viewed with a single profile would appear as evidence of this. However, in spring this pool, which has been maintained throughout the year, largely disappears. This is evidence that either the supply ceases and high rates of diffusion remove the pool within a month, or the diffusion processes accelerate for a period, giving the same result. Regardless, the implication is that high diffusion rates exist deep in the water column. Thus, although the classic turnover processes do not affect this system, hypolimnetic mixing cannot be considered solely driven by molecular processes, and the monimolimnion is not a permanent feature.

Variations in the epilimnion during spring and early summer were expected due to the melting of surrounding snow and ice and also the mine pumping of tailings water. This last factor contributed 80% of the pit-lake volume but must be considered highly site-specific. Despite some of these site-specific factors, the pit-lake provided a useful experimental site to examine vertical diffusion processes. Long-term tracer measurements in conjunction with deep microstructure observations would appear to be the next step, along with improved estimates of the inflows. The tracer measurements will provide a direct quantification of overall diffusion and the microstructure will characterize the associated small-scale physics.

References

CHEN, C.-T., AND F. J. MILLERO. 1977. The use and misuse of pure water PVT properties for lake waters. Nature **266:** 707–708.

DAVIS, A., AND D. ASHENBERG. 1989. The aqueous geochemistry of the Berkeley Pit, Butte Montana, U.S.A. Appl. Geochem. **4:** 23–36.

ELLIS, C. R., H. G. STEFAN, AND R. GU. 1991. Water temperature dynamics and heat transfer beneath the ice cover of a lake Limnol. Oceanogr. **36:** 324–334.

HAMBLIN, P. F., C. L. STEVENS, AND G. A. LAWRENCE. 1997. Vertical transport in Brenda Mines pit lake, p. 367–384. *In* Proc. 4th Intl. Conf. on Acid Rock Drainage, Vancouver, B.C. V. 1.

HEINZ, G., J. ILMBERGER, AND M. SCHIMMELE. 1990. Vertical mixing in Überlinger See, western part of Lake Constance. Aquat. Sci. **52:** 256–268.

HONDZO, M., AND H. G. STEFAN. 1993. Lake water temperature simulation model. ASCE J. Hydrol. Div. **119:** 1251–1273.

JASSBY, A., AND T. POWELL. 1975. Vertical patterns of eddy diffusion during stratification in Castle Lake, California. Limnol. Oceanogr. **20:** 530–543.

KLAPPER, H., AND M. SCHULTZ. 1995. Geogenically acidified mining lakes—living conditions and possibilities for restoration. Int. Rev. Ges. Hydrobiol. **80:** 639–653.

KLOHN LEONOFF LTD. 1986. Brenda Mines abandonment plan: Pit water balance. Report PB 1724-0401. 22 p.

MACINTYRE, S., AND J. M. MELACK. 1985. Meromixis in an equatorial African soda lake. Limnol. Oceanogr. **27:** 595–609.

MARTIN, J.-M. 1985. The Pavin crater lake, p. 169–188. *In* W. Stumm [ed.], Chemical processes in lakes. Wiley.

MCMANUS, J., R. W. COLLIER, C. A. CHEN, AND J. DYMOND. 1992. Physical properties of Crater Lake, Oregon: A method for the determination of a conductivity- and temperature-dependent expression for salinity. Limnol. Oceanogr. **37:** 41–53.

MONISMITH, S. G. 1986. An experimental study of the upwelling response of stratified reservoirs to surface shear stress. J. Fluid Mech. **171:** 407–439.

MÜNNICH, M., A. WÜEST, AND D. M. IMBODEN. 1992. Observations of the second vertical mode of the internal seiche in an alpine lake. Limnol. Oceanogr. **37:** 1705–1719.

NEWMAN, F. C. 1976. Temperature steps in Lake Kivu: A bottom heated saline lake. J. Phys. Oceanogr. **6:** 157–163.

STEVENS, C., AND G. A. LAWRENCE. 1997*a*. The effect of sub-aqueous disposal of mine tailings in standing waters. IAHR J. Hydrol. Research **32:** 1–13.

———, AND ———. 1997*b*. Estimation of wind-forced internal seiche amplitudes in lakes and reservoirs, with data from British Columbia, Canada. Aquat. Sci. **58:** 1–20.

TURNER, J. S. 1973. Buoyancy effects in fluids. Cambridge Univ. Press.

WÜEST, A., W. AESCHBACH-HERTIG, H. BAUR, M. HOFER, R. KIPFER, AND M. SCHURTER. 1992. Density structure and tritium-helium age of deep hypolimnetic water in the northern basin of Lake Lugano. Aquat. Sci. **54:** 205–218.

———, D. C. VAN SENDEN, J. IMBERGER, G. PIEPKE, AND M. GLOOR. 1996. Comparison of diapycnal diffusivity measured by tracer and microstructure techniques. Dynam. Atmosph. Oceans **24:** 27–40.

Received: 16 February 1996
Accepted: 30 December 1997